

Reversible Self-Assembly of Gold Nanoparticles Based on Co-Functionalization with Zwitterionic and Cationic Binding Motifs**

Huibin He,^{*,[a, b]} Kevin Rudolph,^[a] Jan-Erik Ostwaldt,^[a] Jens Voskuhl,^[a]
Christoph Hirschhäuser,^[a] and Jochen Niemeyer^{*,[a]}

Abstract: We report a pH- and temperature-controlled reversible self-assembly of Au-nanoparticles (AuNPs) in water, based on their surface modification with cationic guanidiniocarbonyl pyrrole (GCP) and zwitterionic guanidiniocarbonyl pyrrole carboxylate (GCPZ) binding motifs. When both binding motifs are installed in a carefully balanced ratio, the resulting functionalized AuNPs self-assemble at pH 1, pH 7 and pH 13, whereas they disassemble at pH 3 and pH 11. Further disassembly can be achieved at elevated temperatures at pH 1 and pH 13. Thus, we were able to prepare functionalized nanoparticles that can be assembled/disassembled in seven alternating regimes, simply controlled by pH and temperature.

The stimuli-responsive reversible self-assembly of organic and inorganic materials has a wide range of applications in the field of nanoscience and nanotechnology, for example for optical devices, bio-sensors and in nanomedicine.^[1] For inorganic nanoparticles (NPs), reversible self-assembly can be achieved by introducing surface-anchored ligands that react to external stimuli such as light,^[2] temperature,^[3] pH,^[4] metal ions^[5] or solvent.^[6] For example, the pH-responsive reversible self-

assembly of NPs was achieved by introducing pH-sensitive ligands, such as Brønsted-acids and -bases.^[7] In most cases such pH-responsive systems only possess one switching point, meaning that they self-assemble in one pH-regime and disassemble in a second pH-regime. However, for more sophisticated applications, multiple switching points are highly sought after.^[8]

In principle, such multi-pH responsive behavior can be achieved by using zwitterionic ligands that can assume more than two protonation states. Furthermore, zwitterion-functionalized NPs can show improved biocompatibility and enhanced cellular uptake.^[9] Based on these considerations, we have recently generated zwitterion-functionalized gold nanoparticles (AuNPs),^[10] based on the use of the guanidiniocarbonyl pyrrole carboxylate (GCPZ, Figure 1a) unit that was developed in our group.^[11] GCPZ is a self-complementary binding motif which forms stable dimers in a pH range from 5 to 8, while either protonation or deprotonation led to dimer-dissociation.^[11] The resulting functionalized AuNPs could assemble at neutral pH and disassemble at basic or acidic pH in DMSO/water mixtures.^[10] However, the use of pure water as a solvent remained difficult due to strong hydrophobic interactions, leading to assembly even at low pH, limiting the switchability to two regimes. This was similarly found for other zwitterionic ligands in the literature.^[12]

For this work, we now aim for an improved pH-responsiveness by co-decoration of zwitterion-functionalized NPs with additional cationic ligands. The resulting Coulomb-repulsion could counterbalance attractive hydrophobic interactions in order to enhance the pH-switchability of the assembly/disassembly. In addition, we assumed that the positive charges could assist in an additional temperature-dependent assembly/disassembly,^[13] as recently reported by Grzybowski.^[14]

Initial attempts to use a combination of zwitterionic GCPZ and cationic ammonium ligands did not lead to the desired multi-pH responsive behavior, indicating that the exact choice of cationic co-ligand is crucial. For this reason, we then used cationic guanidiniocarbonyl pyrrole (GCP) ligands as our co-ligands (Figure 1a). In contrast to the GCPZ-motif, the GCP-unit shows a similar pK_a value but lacks the carboxylate unit and is thus positively charged over a wide pH-range.^[11b] When used in a carefully controlled ratio, this combination of ligands resulted in functionalized NPs that could be assembled/disassembled over seven alternating regimes by external stimuli, even in pure water as a solvent.

For the synthesis of the desired co-decorated AuNPs, we prepared AuNPs (mean size 7.2 nm)^[2a] and performed a surface

[a] Dr. H. He, K. Rudolph, Dr. J.-E. Ostwaldt, Prof. J. Voskuhl, Dr. C. Hirschhäuser, Prof. J. Niemeyer
Faculty of Chemistry (Organic Chemistry) and
Center for Nanointegration Duisburg-Essen (CENIDE)
University of Duisburg-Essen
45141 Essen (Germany)
E-mail: jochen.niemeyer@uni-due.de

[b] Dr. H. He
State Key Laboratory of Molecular Engineering of Polymers
Department of Macromolecular Science
Fudan University, 200438 Shanghai (People's Republic of China)
E-mail: huibin_he@fudan.edu.cn

[**] The authors deeply regret the loss of Prof. Dr. Carsten Schmuck, who was a revered scientist, teacher, mentor and friend. Prof. Schmuck was the original supervisor of the project, but as he passed away before it could be finished, J. N. took over supervision.

Supporting information for this article is available on the WWW under <https://doi.org/10.1002/chem.202102457>

© 2021 The Authors. Chemistry - A European Journal published by Wiley-VCH GmbH. This is an open access article under the terms of the Creative Commons Attribution Non-Commercial License, which permits use, distribution and reproduction in any medium, provided the original work is properly cited and is not used for commercial purposes.

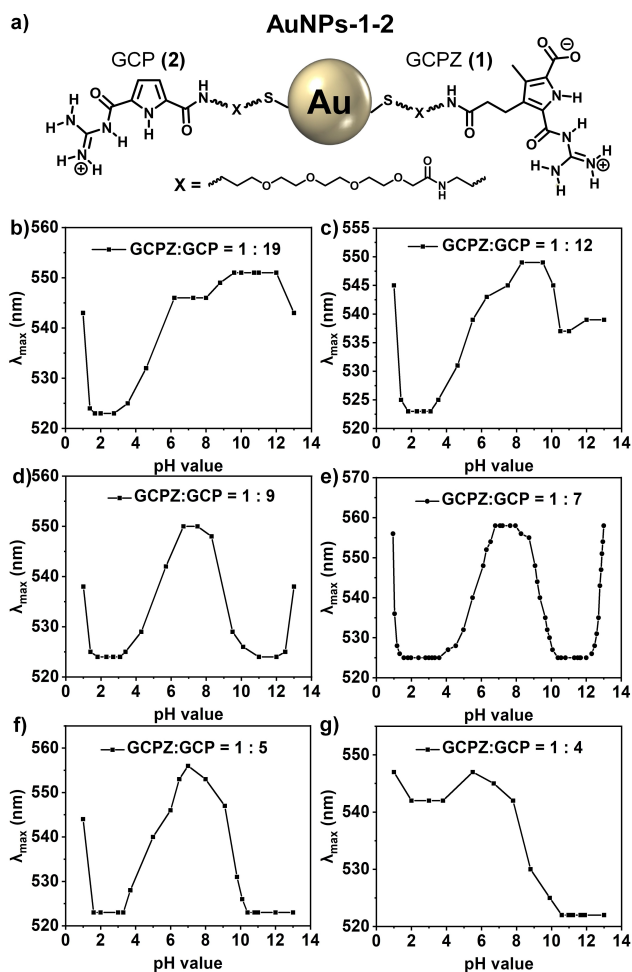


Figure 1. a) Schematic illustration of GCPZ and GCP co-functionalized AuNPs (AuNPs-1-2). b-g) pH-dependent wavelength of absorption maximum of AuNPs-1-2 (68 nM in water) with different GCPZ/GCP ratio, b) 1/19, c) 1/12, d) 1/9, e) 1/7, f) 1/5, g) 1/4.

functionalization using the GCPZ/GCP derivatives (1) and (2) (Figure 1a, see the Supporting Information for details). In the functionalized AuNPs, the GCPZ/GCP-ratio on the NP-surface was found to be approximately equal to the GCPZ/GCP ratio used in the functionalization procedure (Figure S4).

Next, we investigated the self-assembly behavior of these AuNPs using water as a solvent. The assembly/disassembly can be followed by UV/Vis-spectroscopy, since the surface plasmon resonance (SPR) of the dispersed AuNPs (λ_{\max} (disassembled) = ~525 nm) is significantly red-shifted upon self-assembly (λ_{\max} (assembled) = 550–560 nm).

Different ratios of GCPZ/GCP (from 1/19 to 1/4) were used in order to determine the optimal ratio for a pH-induced assembly/disassembly process. With a large excess of cationic GCP (GCPZ/GCP = 1/19), the AuNPs were dispersed in a pH range from 1.5 to 4.0, while self-assembly was observed below pH 1.2 or above pH 4.5 (Figure 1b). When GCPZ/GCP was 1/12, we additionally found partial disassembly in a pH range above 10 (Figure 1c). By further decreasing the excess of GCP (ratio of GCPZ/GCP between 1/9 and 1/7), complete disassembly of the

functionalized AuNPs at $10 \leq \text{pH} \leq 12.5$ was observed (Figure 1d–e), but reassembly occurred at even higher pH (pH 13). Such self-assembly at high pH was suppressed when the GCPZ/GCP ratio reached 1/5 (Figure 1f). Finally, a GCPZ/GCP ratio of 1/4 led to the suppression of disassembly at low pH values (Figure 1g).

From this data, we can draw a couple of interesting conclusions: A) The assembly/disassembly behavior of the co-functionalized AuNPs can be controlled by varying the GCPZ/GCP ratio due to the different pH-responsive properties of GCPZ and GCP. While GCPZ is charged at both acidic and basic pH values, our earlier findings showed that strong hydrophobic interactions between the GCPZ-units are present at neutral, but also at acidic pH. This is due to the presence of the neutral carboxylic acid functionality, which prevents disassembly at low pH.^[10] In contrast, the GCP-unit lacks the carboxylic acid function and thus exhibits a much lower hydrophobic effect than GCPZ. Thus, an excess of the cationic GCP-motif can affect the desired disassembly at low pH-values, while a lower GCP-content mirrors the previously reported behavior^[10] of AuNPs functionalized with GCPZ only (disassembly at high pH values only). B) Using the correct GCPZ/GCP-ratio (from 1/9 to 1/5), we could achieve our initial aim, namely the assembly at neutral pH and the efficient disassembly at lower and higher pH in aqueous solvent. C) We observed reassembly of the AuNPs at very low and high pH-values (pH 1 or 13), most distinctly for a GCPZ/GCP-ratio of 1/7. This was unexpected based on charge repulsion of cationic guanidinium-groups (in GCPZ and GCP at low pH) or anionic carboxylate-groups (in GCPZ at high pH). In summary, we observed five alternating assembly/disassembly regimes, controlled by changing the pH over a range of 1 to 13.

Due to this highly interesting switching behavior, we focused our further investigations on AuNPs with a GCPZ/GCP ratio of 1/7 (referred to as “AuNPs-1-2” in the following). The assembly/disassembly behavior that was observed by UV/Vis (Figure 1e) was confirmed by dynamic light scattering (DLS) measurements (Figure 2b). The hydrodynamic radii of AuNPs-1-2 were in the range of 10 nm at pH 3 and pH 11, which is consistent with the size of disassembled surface-coated AuNPs (ca. 7 nm NP-size + ca. 3 nm ligand size, Figure S1). In contrast, the hydrodynamic radii were larger than 700 nm at pH 1, pH 7 and pH 13, indicating an aggregated state of AuNPs-1-2. Due to the change of the absorption maximum, the assembly/disassembly process could also be followed by naked eye (Figure 2c). Transmission electron microscopy (TEM) showed a similar size distribution at pH 3 and pH 11 and no significant aggregation was observed (Figure 2e/g, see Figure S7–S11 for enlarged images). However, AuNPs-1-2 formed large aggregates at pH 1, pH 7 and pH 13 (Figure 2d/f/h, further characterized by SEM, Figure S18–S21). Notably, no ordered structures were observed in both the TEM and SEM images which might be attributed to the strong attractive interactions between the NPs at pH 1/7/13, leading to rapid and unstructured self-assembly. In summary, the TEM results are in line with UV/Vis and DLS-measurements, confirming the pH-induced self-assembly/disassembly over five alternating regimes.

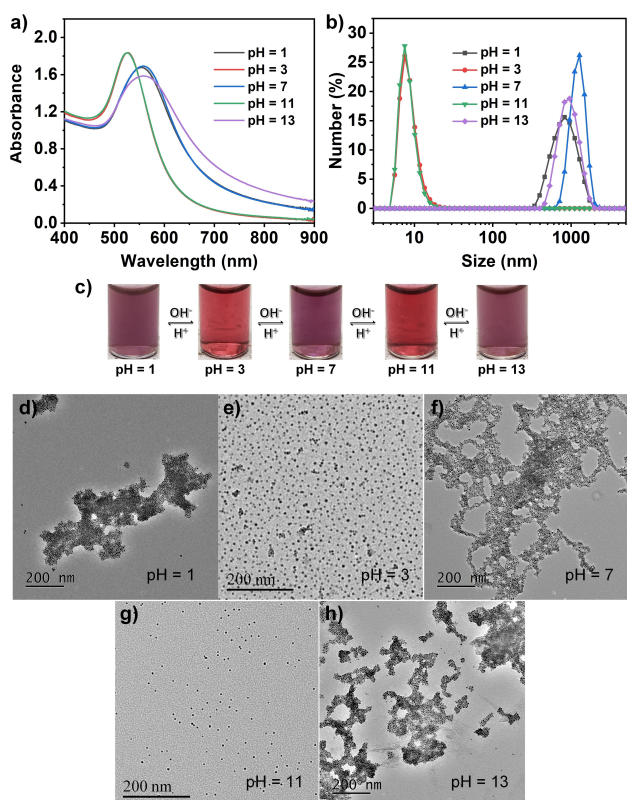


Figure 2. a) UV/Vis absorption spectra, b) DLS measurement and c) photos of AuNPs-1-2 (68 nm in water, GCPZ/GCP = 1/7) at different pH values. d–h) TEM images of AuNPs-1-2 (68 nm in water, GCPZ/GCP = 1/7) at d) pH 1, e) pH 3, f) pH 7, g) pH 11 and h) pH 13 (scale bars different for e/g vs. d/f/h).

Next to pH-induced switching, we investigated whether the self-assembled AuNPs-1-2 could be disassembled by increasing the temperature. While this was not possible at pH 7, we observed a temperature-induced disassembly/reassembly at pH 1 and pH 13. At pH 1, heating up to 70 °C led to a blue-shift of the SPR band from 555 nm to 525 nm, which shifted back upon cooling, indicating full reversibility of the process (Figure 3a/b). This process can also be followed by TEM (carried out by placing cold/hot solutions on the TEM grid, Figure 3e–g, see Figure S12–S14 for enlarged images). At pH 13, the SPR band also underwent a blue-shift from 560 nm to 525 nm upon increasing the temperature to 70 °C. However, in this case cooling to 20 °C resulted in a less pronounced red-shift from 525 nm to 532 nm, indicating only a partial reassembly (Figure 3c/d). This might be caused by the hydrolysis of the GCP-thiolate 2 at high pH and high temperature, which was also found for non-ligated linker 2 in solution (Figure S5). By TEM at pH 13, no complete disassembly was observed either at 70 °C or at 20 °C, possibly due to the presence of large amounts of NaOH after the drying-process (Figure S15–S17). In summary, heating to 70 °C at pH 13 seems to lead to disassembly (according to UV/Vis), but the exact fate of the NPs under these conditions remains unclear.

Next, we investigated the reversibility of the assembly/disassembly process. pH-switching can be repeated more than

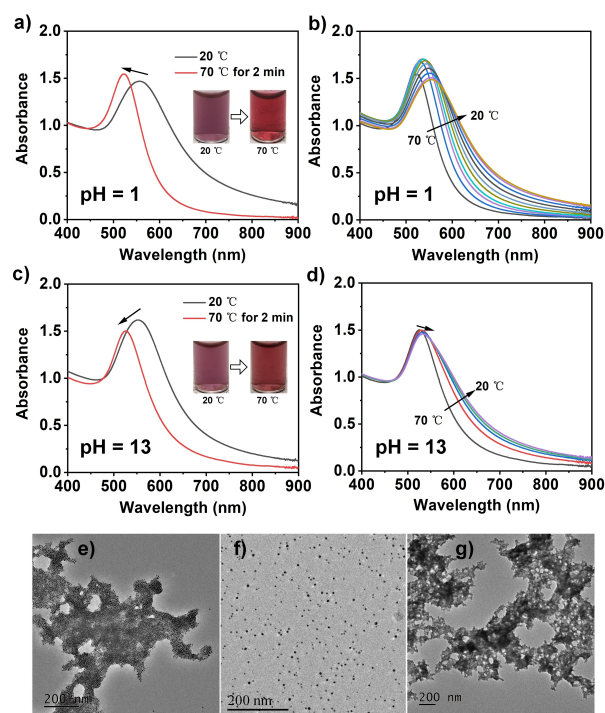


Figure 3. a–d) UV/Vis absorption spectra of AuNPs-1-2 (68 nm in water, GCPZ/GCP = 1/7) at different temperatures, a) pH 1, from 20 °C to 70 °C, b) pH 1, from 70 °C to 20 °C, c) pH 13, from 20 °C to 70 °C, d) pH 13, from 70 °C to 20 °C. e–g) TEM images of AuNPs-1-2 (68 nm in water, GCPZ/GCP = 1/7) at pH 1, prepared at different temperatures, e) 20 °C, f) 70 °C, g) 20 °C, from 70 °C (scale bar different for f vs. e/g).

10 times (between pH 3, pH 7 and pH 11, Figure 4a, also see Figure S23) or even 15 times (between pH 1 and pH 3 or between pH 11 and pH 13, Figure 4b/c). Temperature-induced switching at pH 1 can be repeated more than 20 cycles

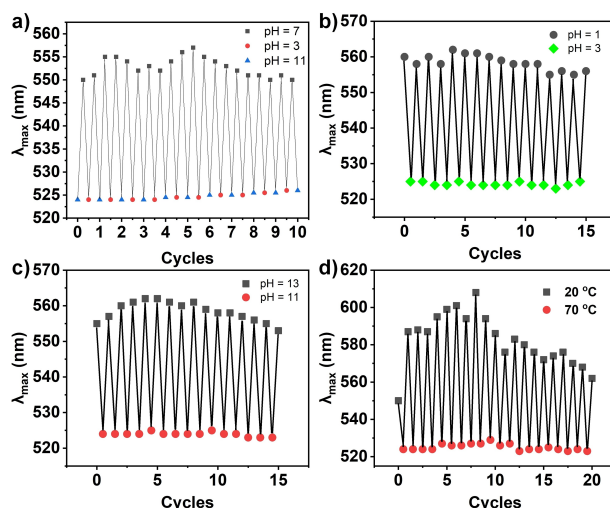


Figure 4. Cycles of reversible self-assembly of AuNPs-1-2 (68 nm in water, GCPZ/GCP = 1/7) between different pH values/temperatures, a) pH 3, pH 7 and pH 11, b) pH 1 and pH 3, c) pH 11 and pH 13, d) at pH 1 between 20 °C and 70 °C.

(Figure 4d). Hence, AuNPs-1-2 show a fully reversible assembly/disassembly (with the exception of the temperature-induced switching at pH = 13, see above).

In order to better understand the mechanism of the pH-induced self-assembly/disassembly, we measured the zeta-potential of AuNPs-1-2 (Figure 5a). AuNPs-1-2 exhibited a zeta-potential of -4 mV at pH 7, while switching to pH 3 or pH 11 led to a change to $+46$ mV (pH 3) or -42 mV (pH 11). Interestingly, going from pH 2 to pH 1 or from pH 12 to pH 13 led to a less positive (22 mV at pH 1) or less negative zeta potential (-29 mV at pH 13). To see if this trend of zeta-potential, which is qualitatively in line with the observed assembly/disassembly behavior (disassembly at pH 3/11, assembly at pH 1/7/13) is unique for AuNPs-1-2, we performed a control experiment with AuNPs-2, which feature GCP-ligands only (Figure 5b). Interestingly, we found a similar trend for the zeta potential, although only three alternating assembly/disassembly regimes were found by UV/vis (assembly at pH 1 and pH > 6, disassembly at pH 2-5, Figure S22a). This clearly shows that electrostatic repulsion alone (estimated by the zeta-potential) is not a sufficient explanation for the assembly/disassembly behavior of AuNPs, neither for AuNPs-1-2, nor for AuNPs-2 (which might be expected to disassemble at high pH based on their zeta-potential).

Our earlier work has shown that weak repulsive charge-interactions can be overcome by attractive dispersion interactions and hydrophobic effects.^[10] This would explain the assembly of AuNPs-1-2 at neutral pH and the missing disassembly of AuNPs-2 at high pH (since no negatively charged ligands are present). However, the question remains why AuNPs-1-2 re-assemble at pH 1 and pH 13 and can be disassembled by increasing the temperature at these pH-values. This might be explained by the influence of ionic strength and temperature on electrostatic repulsion according to the Derjaguin-Landau-Verwey-Overbeek theory. The electrostatic repulsion potential (V_{elec}) between charged NPs is proportional to $\exp(-\sqrt{l})$ (based on ionic pairing with counterions that reduces net-charge) and $\exp(-1/\sqrt{T})$, so that high ionic strength (l) and low temperature (T) lead to a weak repulsion.^[15] Accordingly, we found that addition of NaCl to a solution of disassembled AuNPs-1-2 at pH 3 and pH 11 can trigger their re-assembly (Figure S24), so that self-assembly at pH 1 and pH 13 can most likely be attributed to increased ionic strength. Accordingly, the disassembly at 70 °C at pH 1 or 13 is based on

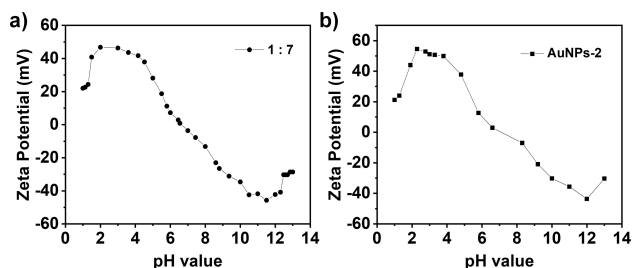
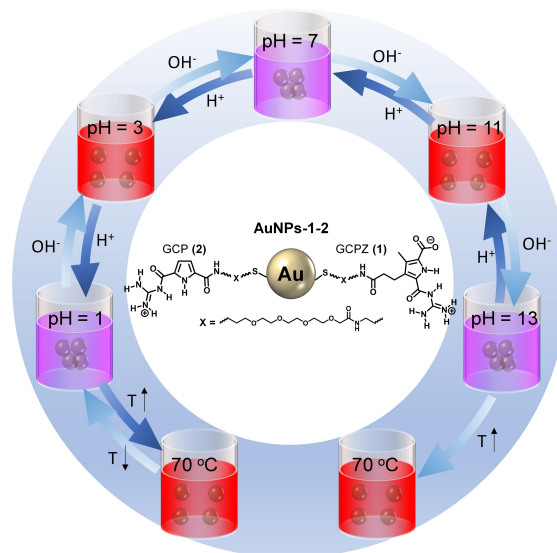


Figure 5. Zeta-potential of a) AuNPs-1-2 (68 nM in water, GCPZ/GCP = 1/7) and b) AuNPs-2 (68 nM in water) at different pH values.



Scheme 1. Schematic representation of the functionalized AuNPs-1-2 and their pH- and temperature dependent reversible self-assembly/disassembly.

an increased electrostatic repulsion at higher temperatures, which is sufficient at low/high pH, while it cannot overcome the stronger attractive interactions at pH 7.

In summary, we demonstrated that AuNPs-1-2 can assemble/disassemble in multiple regimes (Scheme 1). For a finely balanced GCPZ/GCP ratio of 1/7, we found seven alternating assembly/disassembly regimes (Scheme 1), induced by pH and temperature changes. The switching process is fully reversible (except for the reassembly after heating at pH 13 due to hydrolysis) and can be repeated over multiple cycles.

We found that a fine balance of different attractive/repulsive supramolecular interactions, influenced by pH, temperature and ionic strength, is responsible for this unique behavior. Thus, this work gives insights for the future development of novel pH- and temperature-switchable supramolecular systems. For application of our NPs, we are currently investigating the coordination of the GCP(Z) units to specific metal ions such as Hg²⁺ and Cu²⁺, which might allow metal-scavenging by pH-induced co-precipitation, followed by re-dispersion of the NPs to induce re-release of the metal ions.

Acknowledgements

Funding from the DFG (Heisenberg-Professorship to J.N.) is gratefully acknowledged. We thank Evonik Industries AG (funding for J.-E.O.) and the CSC (China Scholarship Council, fellowship for H.H.) for support. We thank Tobias Bochmann and Prof. Matthias Epple for SEM-measurements. We acknowledge the support of the Interdisciplinary Center for Analytics on the Nanoscale (ICAN Duisburg, Germany) for providing the transmission electron microscope used in this work. Open Access funding enabled and organized by Projekt DEAL.

Conflict of Interest

The authors declare no conflict of interest.

Keywords: nanoparticles · pH-responsive · self-assembly · temperature-responsive · zwitterions

- [1] a) B. Dong, S. Du, C. Wang, H. Fu, Q. Li, N. Xiao, J. Yang, X. Xue, W. Cai, D. Liu, *ACS Nano* **2019**, *13*, 1421–1432; b) L. Vigderman, B. P. Khanal, E. R. Zubarev, *Adv. Mater.* **2012**, *24*, 4811–4841; c) G. Yang, J. Nanda, B. Wang, G. Chen, D. T. Hallinan Jr, *ACS Appl. Mater. Interfaces* **2017**, *9*, 13457–13470; d) C. Yi, Y. Yang, B. Liu, J. He, Z. Nie, *Chem. Soc. Rev.* **2020**, *49*, 465–508; e) J. He, X. Huang, Y. C. Li, Y. Liu, T. Babu, M. A. Aronova, S. Wang, Z. Lu, X. Chen, Z. Nie, *J. Am. Chem. Soc.* **2013**, *135*, 7974–7984.
- [2] a) R. Klajn, K. J. M. Bishop, B. A. Grzybowski, *Proc. Natl. Acad. Sci. USA* **2007**, *104*, 10305–10309; b) H. He, M. Feng, Q. Chen, X. Zhang, H. Zhan, *Angew. Chem. Int. Ed.* **2016**, *55*, 936–940; *Angew. Chem.* **2016**, *128*, 948–952; c) P. K. Kundu, D. Samanta, R. Leizrowice, B. Margulis, H. Zhao, M. Borner, T. Udayabhaskararao, D. Manna, R. Klajn, *Nat. Chem.* **2015**, *7*, 646–652.
- [3] a) Y. Liu, X. Han, L. He, Y. Yin, *Angew. Chem. Int. Ed.* **2012**, *51*, 6373–6377; *Angew. Chem.* **2012**, *124*, 6479–6483; b) J. Zhang, P. J. Santos, P. A. Gabrys, S. Lee, C. Liu, R. J. Macfarlane, *J. Am. Chem. Soc.* **2016**, *138*, 16228–16231.
- [4] a) I. Lagzi, B. Kowalczyk, D. Wang, B. A. Grzybowski, *Angew. Chem. Int. Ed.* **2010**, *49*, 8616–8619; *Angew. Chem.* **2010**, *122*, 8798–8801; b) Y. Tan, L. Liu, Y. Wang, J. Liu, *Adv. Opt. Mater.* **2018**, *6*, 1701324.
- [5] a) A. Rao, S. Roy, M. Unnikrishnan, S. S. Bhosale, G. Devatha, P. P. Pillai, *Chem. Mater.* **2016**, *28*, 2348–2355; b) Y. T. Chan, S. Li, C. N. Moorefield, P. Wang, C. D. Shreiner, G. R. Newkome, *Chem. Eur. J.* **2010**, *16*, 4164–4168.
- [6] a) A. Sánchez-Iglesias, M. Grzelczak, T. Altantzis, B. Goris, J. Perez-Juste, S. Bals, G. Van Tendeloo, S. H. Donaldson Jr, B. F. Chmelka, J. N. Israelachvili, *ACS Nano* **2012**, *6*, 11059–11065; b) A. Sánchez-Iglesias, N. Claes, D. M. Solís, J. M. Taboada, S. Bals, L. M. Liz-Marzán, M. Grzelczak, *Angew. Chem. Int. Ed.* **2018**, *57*, 3183–3186; *Angew. Chem.* **2018**, *130*, 3237–3240.
- [7] a) C. Fan, T. Bian, L. Shang, R. Shi, L. Z. Wu, C. H. Tung, T. Zhang, *Nanoscale* **2016**, *8*, 3923–3925; b) J. Ma, Z. Hu, W. Wang, X. Wang, Q. Wu, Z. Yuan, *ACS Appl. Mater. Interfaces* **2017**, *9*, 16767–16777.
- [8] a) P. P. Pillai, S. Huda, B. Kowalczyk, B. A. Grzybowski, *J. Am. Chem. Soc.* **2013**, *135*, 6392–6395; b) M. S. Strozky, M. Chanana, I. Pastoriza-Santos, J. Pérez-Juste, L. M. Liz-Marzán, *Adv. Funct. Mater.* **2012**, *22*, 1436–1444.
- [9] a) T. Mizuhara, K. Saha, D. F. Moyano, C. S. Kim, B. Yan, Y. K. Kim, V. M. Rotello, *Angew. Chem. Int. Ed.* **2015**, *54*, 6567–6570; *Angew. Chem.* **2015**, *22*, 6667–6670; b) H. Wei, N. Insin, J. Lee, H. S. Han, J. M. Cordero, W. Liu, M. G. Bawendi, *Nano Lett.* **2012**, *12*, 22–25; c) Y. Jiang, S. Huo, T. Mizuhara, R. Das, Y.-W. Lee, S. Hou, D. F. Moyano, B. Duncan, X.-J. Liang, V. M. J. A. N. Rotello, *ACS Nano* **2015**, *9*, 9986–9993.
- [10] H. He, J. E. Ostwaldt, C. Hirschhäuser, C. Schmuck, J. Niemeyer, *Small* **2020**, *16*, 2001044.
- [11] a) M. Klein-Hitpaß, J.-E. Ostwaldt, C. Schmuck, M. Giese, *ACS Appl. Polym. Mater.* **2020**, *2*, 2499–2503; b) M. Giese, J. Niemeyer, J. Voskuhl, *ChemPlusChem* **2020**, *85*, 985–997.
- [12] a) E. Moaseri, J. A. Bollinger, B. Chagalvaie, L. Johnson, J. Schroer, K. P. Johnston, T. M. Truskett, *Langmuir* **2017**, *33*, 12244–12253; b) I. I. S. Lim, W. Ip, E. Crew, P. N. Njoki, D. Mott, C.-J. Zhong, Y. Pan, S. Zhou, *Langmuir* **2007**, *23*, 826–833; c) I. I. S. Lim, D. Mott, W. Ip, P. N. Njoki, Y. Pan, S. Zhou, C.-J. Zhong, *Langmuir* **2008**, *24*, 8857–8863.
- [13] a) J. Israelachvili, *Intermolecular & Surface Forces*, Academic Press, London, **1997**; b) H. Zhang, D. Wang, *Angew. Chem. Int. Ed.* **2008**, *47*, 3984–3987; *Angew. Chem.* **2008**, *120*, 4048–4051.
- [14] K. J. M. Bishop, B. Kowalczyk, B. A. Grzybowski, *J. Phys. Chem. B* **2009**, *113*, 1413–1417.
- [15] Y. Wang, G. Chen, M. Yang, G. Silber, S. Xing, L. H. Tan, F. Wang, Y. Feng, X. Liu, S. Li, *Nat. Commun.* **2010**, *1*, 87.

Manuscript received: July 8, 2021

Accepted manuscript online: July 12, 2021

Version of record online: July 29, 2021